LIMNOLOGY and OCEANOGRAPHY: METHODS

Single dual mode (continuous and cast) instrumentation package for inherent optical property measurements: Characterization of the bucket for backscattering observation

Gianluca Volpe [ID],[1]* Davide Dionisi [ID],[1] Vittorio Ernesto Brando [ID],[1] Simone Colella [ID],[1] Jaime Pitarch [ID],[1,2]
Spartaco Ciampichetti,[3] Nicola Ferrara,[1] Gian Luigi Liberti [ID][1]
[1]Istituto di Scienze Marine, Consiglio Nazionale delle Ricerche, Rome
[2]NIOZ, Royal Netherlands Institute for Sea Research, Department of Coastal Systems, Utrecht University, Texel, The Netherlands
[3]Istituto di Scienze dell'Atmosfera e del Clima, Consiglio Nazionale delle Ricerche, Rome, Italy

Abstract

This work describes a continuous sampling system that has been designed, implemented, and tested for the acquisition of Inherent Optical Properties (IOPs) during field campaigns. The major challenge of the work was to design and build a flow-through housing accounting for the complex sensing geometry of the ECO-VSF3, a backscattering meter, i.e., three sensor heads each of which measures the VSF at three angles. A detailed characterization of the ECO-VSF3 housing in terms of impact of the boundaries and overall system inertia is reported. A key feature of the system design is the possibility to easily detach the IOP package from the flow-through hydraulic circuit and use it in cast mode at fixed stations. This, to the best of authors' knowledge, is the first time the ECO-VSF3 is used in an underway system. Results from the comparison of continuous (Co) and cast (Ca) b_b measurements show excellent agreement, with differences not exceeding 7%, thus proving the system to be reliable and highlighting the feasibility for increasing the spatio-temporal sampling of surface observations.

Ocean Colour (in the following OC) aims at understanding the abundance and nature of the seawater constituents by observing the spectral variations of visible light. From the interaction of light with seawater constituents, we are thus able to understand the concentration and sometimes the nature of the particles or solutes that are responsible for the observed radiant field. The radiative transfer equation establishes the link between apparent (AOPs) and inherent optical properties (IOPs). Thus by measuring IOPs, we are able to both predict the light field and obtain key information on the water and its constituents. Here, we focus on the volume scattering function (VSF), which is directly measured via commercial instrumentation and from which we can derive the particle backscattering (b_{bp}).

Satellite OC constitutes a critical component of the Earth observing system. OC contributes to our understanding of the oceanic biogeochemistry by routinely providing global coverage of the surface ocean in terms of phytoplankton biomass and other optically significant water constituents (e.g., colored dissolved organic matter, CDOM, total suspended matter, TSM). Due to the inherent difficulties in generating well-calibrated OC data, OC radiometry requires, more than other satellite remote sensing techniques, accurate in situ measurements in specific environmental conditions (Zibordi et al. 2015) and, as a consequence, adequate in situ programs or infrastructures (e.g., Clark et al. 2003; Antoine et al. 2008; Liberti et al. 2020) for the calibration and validation of the satellite-borne observations. Given well-established measurement protocols (e.g., Banks et al. 2020), accuracy of the in situ radiometric observations allows them to be used as reference to both calibrate and validate remote-sensing observations. However, despite the considerable effort for collecting and harmonizing IOP data from several institutions (Valente et al. 2016), their availability still remains fairly low. Further, this prevents IOP measurement uncertainties to be fully characterized, at least if compared with measurements derived from radiometry. In most cases, station-based measurements on ships provide a poor space–time distribution and are often unable to provide adequate description of oceanographic processes at relevant space–time scales. Increasing data density per-cruise becomes then an important factor that can determine the success of a field campaign not only in relation to the satellite data calibration and validation (CAL/VAL) activities. One way of doing so is to install

*Correspondence: gianluca.volpe@cnr.it

underway systems that allow the measurements to be taken not only at measurement stations but continuously also during navigation (Boss et al. 2019). It is of crucial importance, for the data collected this latter way, to have the same or similar level of accuracy than those collected at stations, adopting well-established measurement protocols. This is surely the case for parameters such as temperature and salinity (Hénin and Grelet 1996) or fluorescence (Lorenzen 1966). In particular, fluorescence is used as surrogate of phytoplankton biomass after being calibrated against phytoplankton pigment concentration measurements such as those derived from high performance liquid chromatography. Although chlorophyll concentration still remains the most widely used and accepted parameter to study phytoplankton biomass distribution and variability, backscattering measurements are progressively becoming more common in the scientific literature (Behrenfeld et al. 2005; Westberry et al. 2008; Martinez-Vicente et al. 2013; Bellacicco et al. 2019). The latter offers the advantage of being less sensitive to photo-acclimation, a process for which phytoplankton cells change their chlorophyll content as function of light and nutrient availability without any significant change in biomass (Behrenfeld and Boss 2003; Bellacicco et al. 2016). In addition, b_b is also directly related to water turbidity and particle size distribution (Loisel et al. 2006; Kostadinov et al. 2009). Particle backscattering in continuous systems has already been successfully retrieved by measuring the volume scattering function at one central angle of about $117°$, $\beta(117°)$ $(m^{-1}\ sr^{-1})$, with a WET Labs ECO-BB3 sensor at three wavelengths: 470, 526, and 656 nm, with 1 Hz sampling rate (Dall'Olmo et al. 2009). To operate the ECO-BB3 instrument continuously, Dall'Olmo et al. (2009) used a custom-made flow-through chamber (8.7 L volume), whose impact on the measurement was characterized by laboratory replicates over a relatively wide optical absorption range. This characterization experiment yielded a relatively constant perturbation from the chamber walls to the b_b measurements, which was treated as an offset and removed from the cruise data. Their work was based on the reasonable hypothesis that the chamber does not degrade during the cruise. However, the way most of the underway systems are conceived prevents from monitoring data quality during the cruise (Boss et al. 2019). The ideal would be to periodically deploy the instrument used in the underway system for taking measurements in cast mode so that any system issue can be addressed in a timely manner. What prevents the same instrument to be used also in cast mode is the entire system setup that should be sufficiently versatile to allow it.

The goal here is to increase the surface space–time data density using a flow through continuous sampling system for IOP measurements, while maintaining an accuracy comparable to the one associated with cast measurements. In this study, we explore the feasibility to achieve this goal by demonstrating that a versatile system setup does allow the deployment, at stations, of the same set of instruments used underway. One dual mode configuration instrument package for continuous (Co) and cast (Ca) IOP data acquisition, the CoCa system, has been designed

and developed and it is here described. Thus, the CoCa system, in principle, ensures full compatibility between the two types of acquisition providing the opportunity to operate a single IOP package to explore both the surface horizontal variability during navigation as well as the depth variability in correspondence of the station operations. Moreover, the use of the same instrumentation in both modes allows a more prompt readiness to system degradation, e.g., due to microbubbles or fouling into the hydraulic underway system.

The major challenge of this work is to design, build, and characterize a flow-through housing accounting for the complex sensing geometry of the ECO-VSF3 (Sullivan et al. 2012), i.e., three sensor heads each of which measuring the VSF at three angles. In this work, we will focus on the characterization of the seawater container that was designed and built for the underway VSF measurements, via the ECO-VSF3 instrument (WETLabs, Inc.). This container will be hereafter referred to as b4bbo (bucket for b_b observations).

The aim of this work is to evaluate the CoCa system accuracy by associating the continuous measurements with the uncertainty estimated by comparison with the cast measurements or, in case, by identifying suitable data processing corrections. Next section provides all necessary elements for building b4bbo along with the details for setting up the system for its successful operation on a ship. The system characterization is made of both laboratory and field experiments which were meant to assess the behavior of b4bbo and of the CoCa system.

Methods

This section introduces the cruise in which the system was implemented and tested, leading to the optimal final configuration. The section continues with a description of the instrumentation package, of the b4bbo design and of the CoCa system configuration. The analysis shown in Section 2 relies on the statistical parameters of Table 1.

The cruise

The BioOpt 2019 cruise took place from the 7th May to the 4th June 2019 across the western Black Sea on board the R/V Akademik of the Bulgarian Academy of Science. The objective of the cruise was to characterize the bio-optics of the area by using radiometry and IOP measurements and by collecting water samples for filtration and subsequent laboratory analysis. Station measurements were performed only during daytime and the IOP package was used in cast mode at the first and last stations of the day to characterize the continuous measurements. Figure 1 shows the spatial distribution of the b_b casts acquired during the cruise. The underlying map is the overall average chlorophyll concentration during the cruise period estimated from the multisensor Level-3 daily product optimized for the Black Sea by CMEMS (Copernicus Marine Environment and Monitoring Service, https://marine.copernicus.eu). The map shows that the spatial distribution of the stations encompasses different trophic

Table 1. Statistical parameters used in this study to estimate the uncertainty associated with the CoCa system. Co and Ca stand for continuous and cast measurements, $(\bar{Co})$ and $(\bar{Ca})$ being their averages, respectively.

$$Slope = \frac{1}{2\sum_{i=1}^{N}(Co_i - \bar{Co_i})(Ca_i - \bar{Ca_i})}\sum_{i=1}^{N}(Co_i - \bar{Co_i})^2 - \sum_{i=1}^{N}(Ca_i - \bar{Ca_i})^2 +$$

$$\left\{ \left[\sum_{i=1}^{N}(Co_i - \bar{Co_i})^2 - \sum_{i=1}^{N}(Ca_i - \bar{Ca_i})^2\right]^2 + 4\left[\sum_{i=1}^{N}(Co_i - \bar{Co_i})(Ca_i - \bar{Ca_i})\right]^2 \right\}^{\frac{1}{2}}$$

$$Intercept = \bar{Co} - Slope \cdot \bar{Ca}$$

$$r^2 = \frac{\left[\sum_{i=1}^{N}(Co_i - \bar{Co_i})(Ca_i - \bar{Ca_i})\right]^2}{\sum_{i=1}^{N}(Co_i - \bar{Co_i})^2 \sum_{i=1}^{N}(Ca_i - \bar{Ca_i})^2}$$

$$RMSD = \sqrt{\frac{\sum_{i=1}^{N}(Co_i - Ca_i)^2}{N}}$$

$$bias = \frac{1}{N}\sum_{i=1}^{N}(Co_i - Ca_i)$$

$$RPD = 100 \cdot \frac{1}{N}\sum_{i=1}^{N}\frac{Co_i - Ca_i}{Ca_i}$$

$$APD = 100 \cdot \frac{1}{N}\sum_{i=1}^{N}\frac{|Co_i - Ca_i|}{Ca_i}$$

regimes. Temperature, salinity and fluorescence values measured during CTD casts were clustered according to the satellite chlorophyll concentration (Table 2) into three roughly homogeneously distributed sample groups. The three trophic regimes translate into three different optical conditions. The off-shore oligotrophic blue waters in the south-western sector are characterized by high temperature and salinity and low fluorescence values (Table 2); on the opposite, low temperature and salinity and high fluorescence values characterize the area off the Danube Delta. Intermediate conditions are encountered for the other measurement stations.

IOP package

The IOP package consists of three instruments:

(1) A CTD (Conductivity Temperature Depth) MicroCAT SBE-37-SI, from Sea-Bird Scientific to provide the necessary depth reference along with temperature and salinity data that are also needed to correct ACs measurements.

(2) An ACs from WetLabs, measuring the light absorption (a) and attenuation (c) at 83 spectral bands, regularly distributed between 400 and 740 nm. In both cast and continuous mode, the water flows through the c-tube first and then into the a-tube.

(3) An ECO-VSF3 from WetLabs, measuring the volume scattering function at three wavelengths (470, 532, and 660 nm) and three nominal angles centered at 100°, 125°, and 150° with the full width half maximum bandwidth of about 18°.
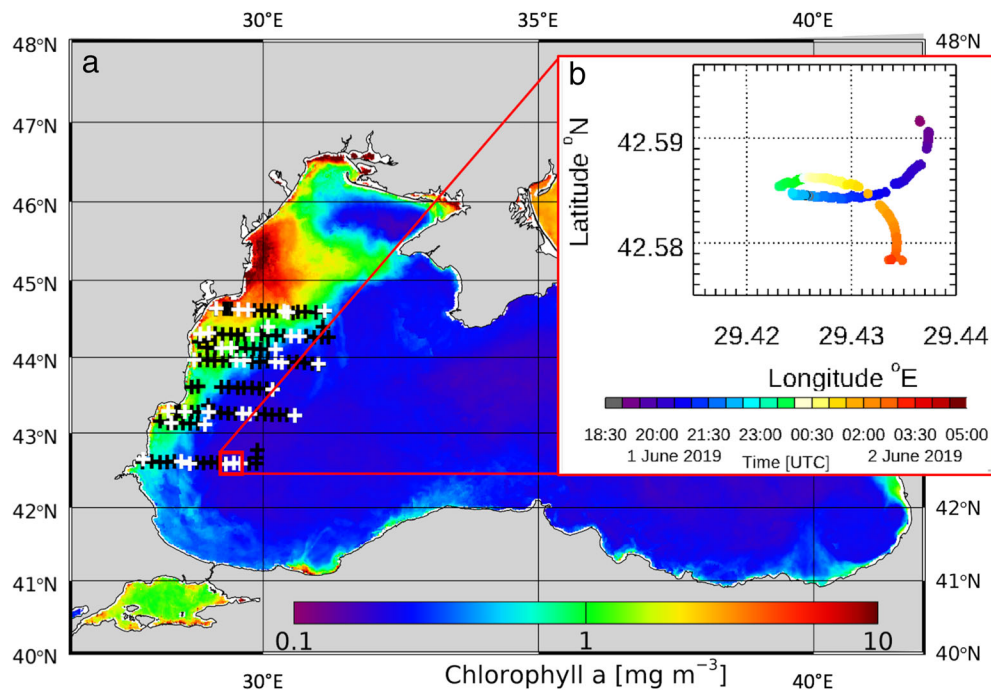

Fig 1. Panel (**a**): Spatial distribution of b_b profiles (white crosses) acquired during the BioOpt 2019 cruise (7th May—4th June 2019) superimposed to the chlorophyll concentration average map estimated for the cruise period. Chlorophyll concentration average is computed from the multi-sensor Level-3 product available from the Copernicus web site (http://marine.copernicus.eu). Black crosses identify the location of all the stations sampled during the cruise and from which the values of Table 2 were derived. Panel (**b**): Location of the ship during the experiment to determine the system inertia (*see* Section 2.2.1 for more details); colors identify the time of the day (UTC).

Table 2. Values computed from the top 10 m of all the CTD casts performed during the cruise (black crosses in Fig. 1a) and clustered according to the three satellite-derived chlorophyll ranges (top row; Chl units are mg m^{-3}).

	0.01 ≤ Chl < 0.35 (N = 47)			0.35 ≤ Chl < 1 (N = 41)			1 ≤ Chl < 20 (N = 45)		
	Min	Aver	Max	Min	Aver	Max	Min	Aver	Max
Temperature (°C)	11.88	17.98	21.32	10.53	16.50	21.56	9.09	15.65	21.57
Salinity (psu)	17.23	18.28	19.28	16.03	17.66	19.09	9.69	16.74	18.30
Fluorescence (mg m^{-3})	0.089	0.401	0.882	0.089	0.802	4.546	0.302	2.881	14.099

(4) A four-ports data handler (DH4) from Sea-Bird is used to connect the instrumentation to a computer for real-time data transmission and visualization. DH4 was modified by adding an extra input/output connection to allow switching off the pump and the CTD during continuous measurements.

A steel frame hosts the instrumentation along with a submersible pump (Sea-Bird Scientific SBE 5T) to let seawater through the CTD and the ACs when the frame is deployed and used underwater in cast mode. This pump only works for the cast mode and is turned off when the package is operated on board in continuous mode and a dedicated on-deck diaphragmatic pump (Graco Husky 1050E pump) is switched on (Fig. 2).

A full description of the ECO-VSF3 sensor and of the principle of the measurement can be found at the ECO-VSF 3 User's Guide (https://www.comm-tec.com/prods/mfgs/wetlabs/manuals/eco-vsf3_manual.pdf). Briefly, ECO-VSF3 sensor consists of three heads for measuring the VSF at three wavelengths. Each head is equipped with one emission source for each of the three angles and one detector. To minimize the impact of the emission sources of each head, these point outward, as shown by the schematics of the acquisition measurement (Fig. 3a). The emission angles have been shown to actually be 111°, 138°, and 154° (Michael Twardowski personal communication), rather than those declared by WetLabs. To minimize ship vibration to perturb the measurement by introducing spurious variability, during navigation the IOP package is placed on a 10 cm high foam panel.

b4bbo design

The bucket for backscattering observation, b4bbo, is made of black-painted 3 mm thick aluminum sheet. One relevant aspect to consider is the effect on measurements by reflection from its internal surfaces. This has strong implications for the quality of the data acquired in continuous mode. b4bbo internal surface coating is glossy to allow specular reflection toward the bottom. To test the fitness for purpose of the b4bbo internal coating, the reflectance of its internal surfaces was measured using an ASD spectroradiometer (ASD FIELD SPEC PRO 350–2500 nm; https://fsf.nerc.ac.uk/instruments/asd_fieldspec.shtml) in dry conditions. Reflectance measurements ranged from 2.78% for the 650 nm band, to 2.91% for the 532 and 2.97 for the 470 nm. The low reflectance values give

us confidence that the material used to build b4bbo is adequate and fit for purpose. However, relating measurements performed in dry and wet conditions is not straightforward as water refractive index changes the direction of light propagation. The following analysis will mostly deal with the impact of b4bbo shape and dimensions on the continuous measurements.

To ease its construction, painting of the inner surface as well as to allow daily cleaning and maintenance, b4bbo was made of two parts (Fig. 3b), which are adhered to one another by four clamps, easy to operate. A gasket between the two prevents leakage.

The volume of b4bbo was determined as a trade-off between the need of making the container small to reduce system inertia and dilution effect and, on the opposite side, the need of making it large to minimize the influence of its internal surface in b_b. Thanks to its shape, b4bbo volume is only 7.9 L, similar to the 8.7 L of the custom-built b_b casket from Dall'Olmo et al. (2009).
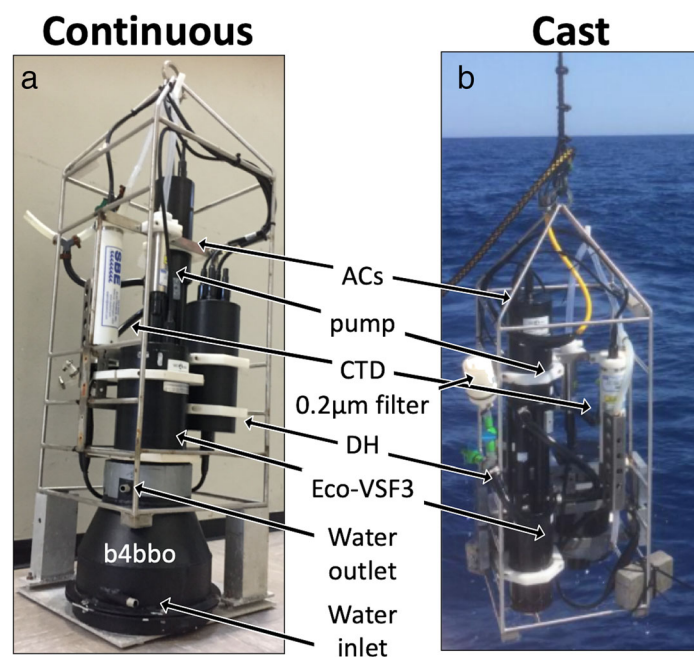
Fig 2. Pictures of the IOP package when operated in continuous (panel **a**) and cast (panel **b**) modes, with sensors being labeled.
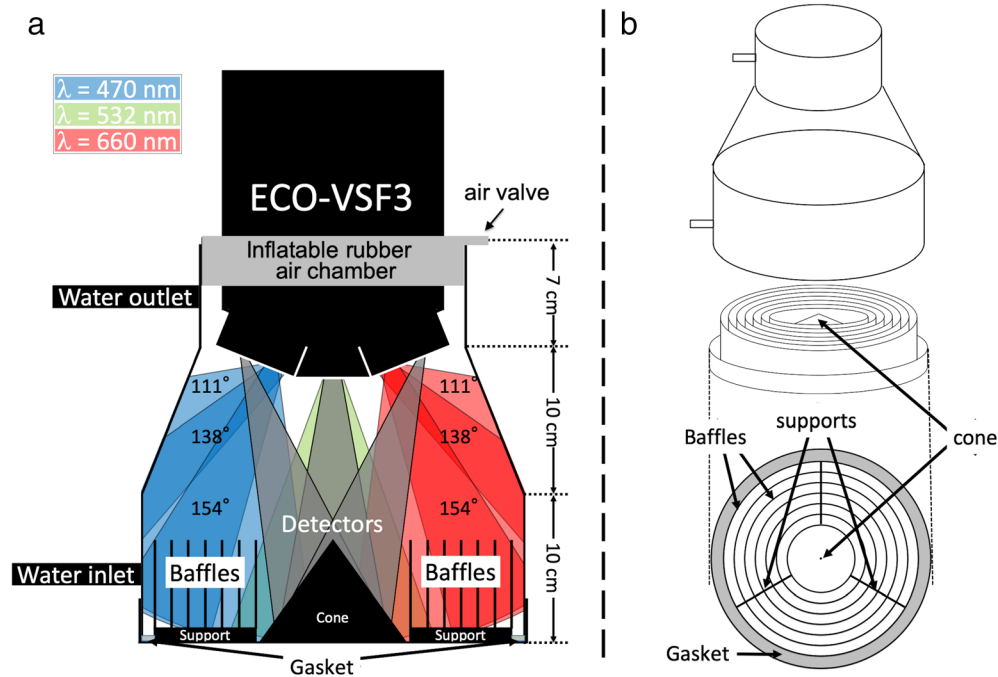
Fig 3. Panel (**a**): Schematic representation of the VSF measurement within b4bbo, showing the three sensor heads responsible of the three-band emission and measurement (470, 532, and 660 nm), each at three angles (111°, 138°, and 154°). The field of view of the instrument heads is shown in gray. Panel (**b**): b4bbo is made of black-painted aluminum and consists of two parts; the upper part is made to adhere to the ECO-VSF3 instrument through the inflatable rubber air chamber and the lower part contains the baffles to trap the light emitted by the ECO-VSF3 sensor.

To reduce the effect of the internal reflections of the light pulses emitted by the ECO-VSF3, a light trap was created on the bottom of the chamber. The first design of the light trap consisted of seven 6 cm high concentric baffles, spaced 1 cm and perpendicular to the bottom plane (Fig. 3). However, when compared with measurements obtained in cast mode, this design still resulted in significant overestimation of b_b reasonably due to back-reflection by the bottom of the chamber of the 154° beam to the sensor detectors (Volpe et al. 2018). The final design includes a cone the same height as the baffles in the center of b4bbo bottom (Fig. 3). This configuration provided better results (*see* Section 2.2.2). To further reduce the impact of the lateral internal surface over VSF measurements, the upper part of b4bbo was given the shape of a truncated cone. The slanting internal surface promotes the specular reflection of the beams away from the sensor detectors and toward the light trap at the bottom. This reflection affects the backscattered beams at 111°, 138°, and 154° in decreasing order.

The upper cylindrical part of the container (7 cm height) is used to place the ECO-VSF3 sensor. An ad hoc inflatable rubber air chamber is used for both sealing the VSF meter to b4bbo and to reduce ship vibration contamination. In a future upgrade, we foresee the use of a gasket custom made out of liquid rubber.

The three baffle supports, 1 cm high are spaced 120° from each other. The water intake is tangential to the lateral surface of the lower cylinder of b4bbo, to reduce the turbulence within the container and its impact on the VSF measurement. This design allows for an efficient water recirculation in the space among the baffles thus reducing the inertia of the continuous measurement.

The CoCa system

For the system to be operated in continuous and cast modes and to reduce the risks of instrument damage, the distance between the continuous mode location and the winch for profiling must be minimized as much as possible. When the steel frame is not deployed into the water, it is placed into b4bbo, which is embedded into an ad hoc support that allows the frame to be secured during ship operations and navigation. During BioOpt 2019, b4bbo support was placed on the floor of the wet laboratory over a 10 cm foam panel to reduce vibrations and to avoid physical strain in lifting the IOP cage. In cold waters ($T < 10°C$), the ACs lens tend to fog, greatly reducing their sensitivity. One solution would be to immerse the ACs meter in its sampling water: this would require further refinements to the CoCa system. However, such low water temperatures were never met during flow-through measurements and only rarely approached during cast measurements (Table 2).

The schematics of the on deck flow-through system for IOP measurements is shown in Fig. 4b. Roughly located in the

center of the ship to reduce wave influence, a steel pipe was attached to the ship wall (Fig. 4a) and served as support for a semirigid PVC tube, used to collect water from 1 m below surface (in calm sea conditions). In our case, to fix the steel pipe we only had one anchor point over the ship deck; this was clearly not enough to secure the steel pipe. To prevent damages to the system and to the ship, especially during navigation, the steel pipe was roped from bow and stern after having placed a boat fender close to the sea surface between the steel pipe and the ship wall; this resulted in very efficient suppression of vibrations (Fig. 4).

The semirigid PVC tube was connected to an electrically operated diaphragmatic polypropylene pump, which is also able to modulate the flow rate. It is worth noting that during the entire cruise, thus also during the cast mode, the flow-through pump was always on, except for daily system cleaning, which generally lasted no more than 30 min, every day. Keeping the pump on also during casts reduces the time required for the system to be brought up and running back again. A PVC tube conducts the seawater from the pump toward two vortex de-bubblers (6 cm diameter, 25 cm height, Ocean Instrument Laboratory), set in series, to remove the impact that air bubbles have on the optical measurements. An electro-valve, which can be operated both automatically and manually, forces the flow through a 0.2 μm filter (AcroPak 1000 Supor Membrane, from Pall Corporation) or directly into the ACs meter. This enables the contribution of seawater and dissolved matter (CDOM) to the absorption and attenuation to be estimated and removed from total

a and c measurements. The limited size (1350 cm^2) of the current filters translates into a substantial reduction of the water flow into the system (*see* Section 2.2.1). To estimate the particle contribution to total absorption and attenuation measurements also when the system is operated in cast mode, two consecutive casts are made, with and without particle filter (Fig. 2). A commercial flowmeter (1/2″ Water Flow Sensor for Arduino with a flow rate between 1 and 30 L/min—manufacturer reference: Keenso35t78wbfdn) is located upstream of all the instrumentation to monitor the system conditions and to support data interpretation when field measurements change without any apparent reasons (Boss et al. 2019). All parts of the system are interconnected by black Tygon tubing (1.3 cm diameter), except the part from the sea surface to the pump, and from the pump to the de-bubblers which is made of semirigid PVC tubes (1.73 cm diameter). However, having some components of the hydraulic circuit made by transparent pipes allows routinely checking for the presence of air bubbles. For example, it is very useful when the 0.2 μm filter cartridge has to be replaced, operation that generally takes a few minutes before all the bubbles are removed. One such part is the first half of the tube connecting the flow-meter and the ACs meter. Here, the seawater first enters the c-tube and then the a-tube. b4bbo is located right downstream of ACs. The second half of the tube connecting the ACs meter and b4bbo is also transparent. To ensure b4bbo is constantly full of water without any residual air, its drain tube must be placed higher than b4bbo water outlet exerting a backpressure that eases air bubble removal. However, if the measured VSF
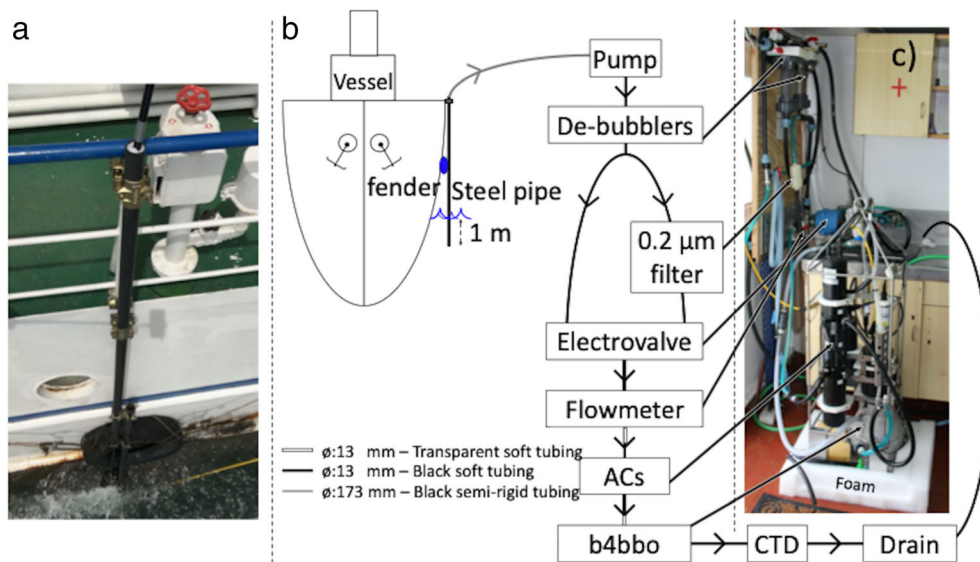

Fig 4. Panel (**a**) shows a picture of the steel pipe clamped on the ship wall. Panel (**b**) schematics of the flow-through system with the water flowing, following the arrows, from the 1 m below surface, through the steel pipe, the pump, the de-bubbling system. Here, an electrovalve allows the water to either going directly into the ACs meter or passing through the 0.2 μm filter, first. b4bbo is located downstream of the ACs meter over a 10 cm foam panel. The water then is redirected to drain where a CTD instrument is located. The two pictures refer to the system installed on the R/V Akademik during the BIO-OPT 2019 cruise. Panel (**c**) shows a picture of the wet laboratory where the flow-through system was installed.

Table 3. Estimation of water volumes in each component of the flow-through system (last column) as it was installed on the R/V Akademik during BioOpt 2019 cruise. The first two columns refer to the starting and ending points connected by the tubes whose section and length is shown in the third and fourth columns. The filter path length and volumes, in parenthesis, include the 0.2 μm filter volume of 0.18 L.

From	To	Section (cm^2)	Length (cm)	Volume (L)
Surface water	De-bubbler # 1	2.35	2680	6.3
De-bubbler # 1	De-bubbler # 2	2.35	162	0.38
De-bubbler # 2	Flowmeter (filter path)	1.33	99 (157)	0.13 (0.39)
Flowmeter	c-tube	1.33	148	0.20
c-tube		1.13	24	0.03
c-tube	a-tube	1.33	46	0.06
a-tube		1.13	24	0.03
a-tube	b4bbo	1.33	167	0.22
b4bbo		–	–	7.9
b4bbo	CTD	1.33	282	0.38
Total				15.63 (15.89)

signal is unphysical and not imputable to air bubbles, then it is very likely that the system has to undergo cleaning and maintenance.

If the length and diameter of the tubing system are measured precisely, the volume of water into the system at any time can be calculated. This, associated with the vessel speed, allows the accurate geolocation of the continuous measurement. The volumes of water involved into the system when operated in continuous mode are detailed in Table 3.

During continuous measurements, the pressure exerted by seawater flow (approx. 2–10 L/min) requires the frame with all the instruments to be fixed to its support and b4bbo. To take the cast measurements and to let the steel frame out of b4bbo, the inflatable rubber air chamber has to be deflated. In regular operation, casts can reach depths of 70 or 80 m. However, to validate the continuous measurements, it is convenient to acquire cast observations from the same depth as the water intake (in this case 1 m depth) for at least 3 min. The 3-min data collection (roughly 180 measurements) enables the computation of statistically robust mean values and associated standard deviation to be used for comparison with the continuous measurements.

Figure 4b shows that the CTD is placed downstream b4bbo. However, given the involved volumes of water (Table 3), b4bbo's inertia is obviously larger than most other instruments' (*see* Section 2.2.1), so that it would be better for the CTD (or any other additional instrument that does not affect b_b measurement) to be placed upstream b4bbo.

For the purpose of this work, only ECO-VSF3 data were analyzed. Attenuation coefficients derived by ACs measurements were used onboard to qualitatively visualize the effective switch between total and filtered waters through the system, as shown later in Section 2.2.1. Since the objective is
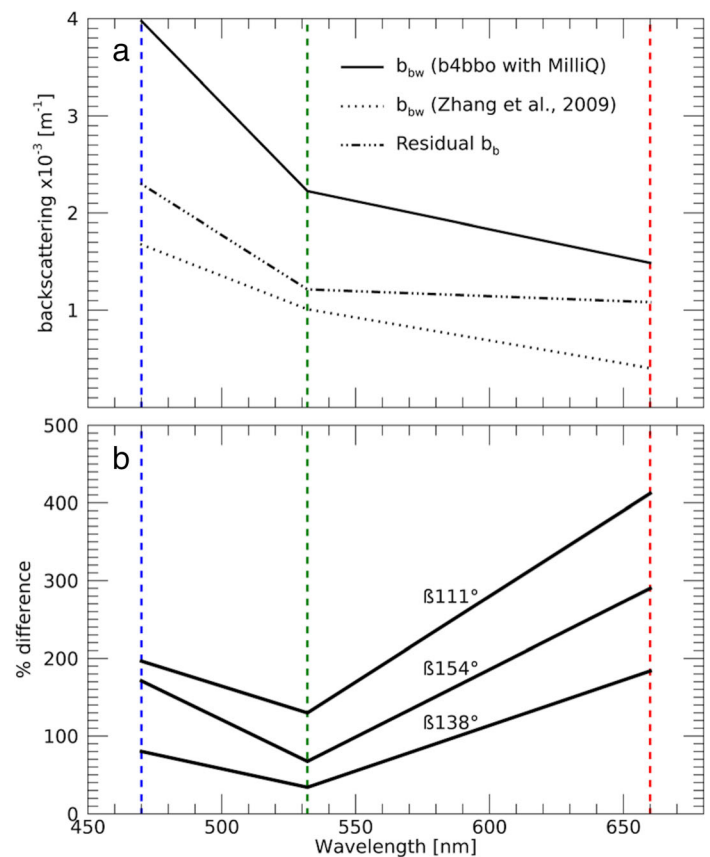

Fig 5. (**a**) Average bb spectrum obtained with the ECO-VSF3 measuring the MilliQ water into b4bbo (continuous line). As reference the half scattering of the pure water (Zhang et al. 2009) is also shown as dashed line. The difference between the two is shown as long-dashed line. As a reference, in both panels, vertical dashed and colored lines show the ECO-VSF3 wavelength bands. (**b**) Difference (%) between the volume scattering function derived from the MilliQ water measurement within b4bbo and that derived from Zhang et al. (2009).
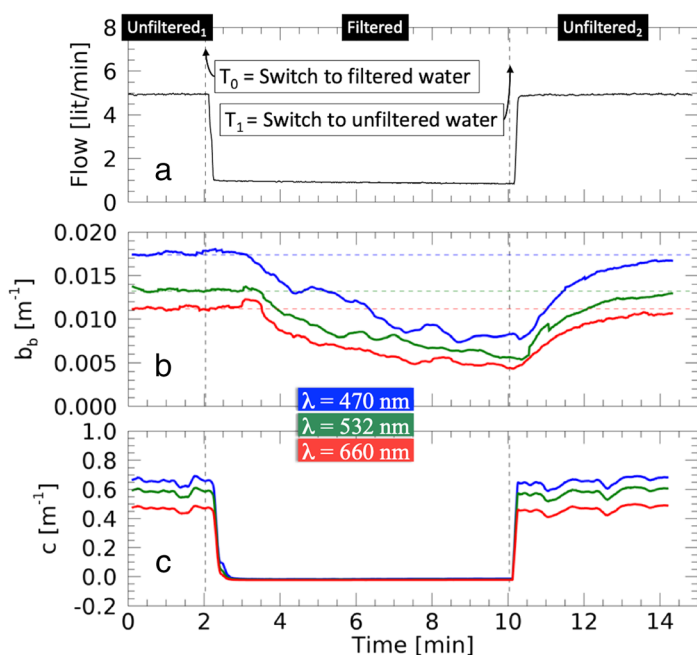
Fig 6. Example of measurement for the estimation of system inertia taken the 1st June 2019 at 18:30 UTC. Panel (**a**) Seawater flow measured upstream of the c-tube of the ACs. Panel (**b**): Example of continuous b_b measurement to determine the rate of change of the water inside b4bbo. Panel (**c**): Same as panel (**a**) but for the attenuation coefficient of light, without the water contribution, at the same wavelength as b_b. In both panels, colors identify the wavelength (nm, *see* inlet). The vertical dashed lines indicate the time of the electrovalve activation to switch to filtered water (first dashed vertical line, denoted as T_0) and to unfiltered water again (second dashed vertical line, denoted as T_1). These identify the three areas in the plot indicated as unfiltered$_1$, filtered, and unfiltered$_2$, which lasted 2, 8, and 4 min, respectively. VSF and c data were smoothed with a running mean of 30 s, while flow data were smoothed at 4 s. Data used in this figure can be accessed at 10.5281/zenodo.4564781

to evaluate b4bbo capability to retrieve reliable b_b measurements in continuous mode, and that data were tested against cast mode acquisitions, no data postprocessing is here applied to the VSF data. The rationale is to compare measurements acquired in two different modes uniquely applying manufacturer calibration.

Results and discussion

This section describes the CoCa system characterization and is split into two subsections that present the laboratory and field work, respectively. Laboratory analysis mostly concentrated on the characterization of the b4bbo internal surface using MilliQ water. Since b4bbo accounts for half the entire system water volume, field experiments were carried out to characterize b4bbo inertia due to dilution. Moreover, to check the overall quality of the continuous measurements, Section 2.2.2 presents the comparison with the cast mode measurements.
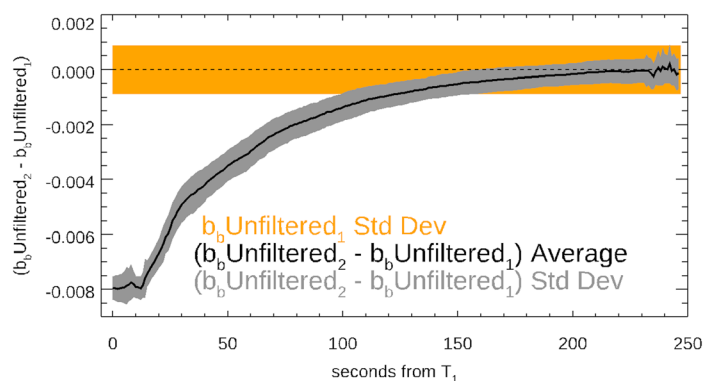

Fig 7. Estimation of seawater residence time into b4bbo. Black line and the gray-shaded area are average and standard deviation of the differences between b_b (Unfiltered$_2$) and b_b (Unfiltered$_1$) computed among all the 16 independent experiments described in Fig. 6. The orange shaded area is the standard deviation of the b_b (Unfiltered$_1$). Data used in this figure can be accessed at 10.5281/zenodo.4564781

Laboratory measurement with MilliQ water

Figure 5a shows the average b_b spectrum obtained with the ECO-VSF3 measuring the MilliQ water into b4bbo. To prevent micro-bubbles affecting the measurement, the MilliQ water was left still for 12 h in complete darkness. However, this kind of measurements is very challenging as it requires a clean room to prevent any possible source of contamination; unfortunately, this test was performed in a normal wet laboratory. The residual difference between MilliQ water measurements with b4bbo and the theoretical backscattering of pure water (Zhang et al. 2009) highlights the small yet non-negligible contribution of the b4bbo itself to b_b measurements (Fig. 5). In these conditions, for which the internal surfaces apparently account for as much as the pure water for the blue and green bands and twice as much in the red band, the contamination by non-ideal ambient laboratory conditions could play a role or at least be considered as contributing to it. The largest relative contribution to this discrepancy comes from the 111° and 154° measurements for which the light trap within b4bbo appears to be less efficient (Fig. 5b). Given that the effect of the walls decreases with water turbidity, this can be considered as the upper limit uncertainty that we can reasonably expect for the CoCa system.

Field experiments

System inertia: Water residence time

The b4bbo round shape and the tangential water intake (Fig. 3) are meant to favor the water recirculation within b4bbo and its water renewal time. The renewal time associated with the speed of the research vessel defines the system sampling characteristics. Our minimum goal, here, is to resolve at least the 1 km scale, which is the finest spatial resolution of Ocean Color data available from the Copernicus Marine Service (http://copernicus.marine.eu) or from the Ocean Biology
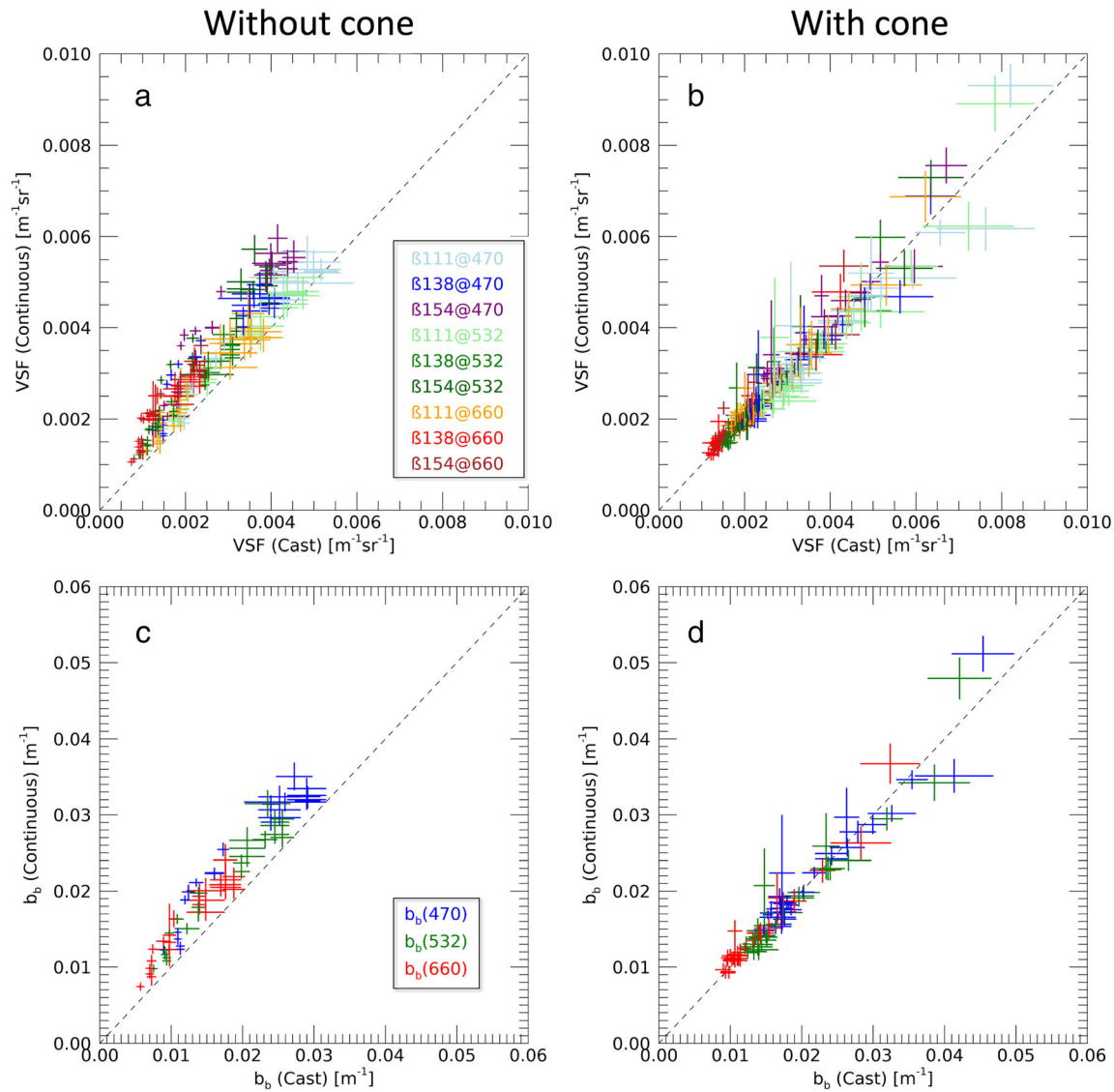
   Volpe et al.

Fig 8. Comparison of continuous and cast mode for VSF (panels **a** and **b**) and bb (panels **c** and **d**). Continuous mode measurements acquired without the cone (**a** and **c**, 7–23 May 2019) and with the cone (**b** and **d**, 24 May–6 June 2019). Error bars are the standard deviation of cast and continuous measurements lasting 3 min. Data used in this figure can be accessed at 10.5281/zenodo.4564781

Group at NASA (http://oceancolor.gsfc.nasa.gov). Thus the estimation of the residence time is crucial to determine the underway system spatial resolution.

To estimate the system spatial sampling characteristics, a set of 16 independent acquisitions was performed using filtered and unfiltered seawater. The experiment was conducted during the BioOpt 2019 cruise (Fig. 1) during an entire night in which the ship was left adrift. The calm sea conditions allowed the ship to be virtually kept at the same location (Fig. 1b) over the experiment period. Thus, at the scale of each of the 16 acquisitions (14 min each), the optical variability of the water can be considered negligible. On the other hand, the variability within the whole set of acquisitions is taken into account and ensures a robust, consistent and reference statistics.

Every half an hour, data acquisition started with the b4bbo full of unfiltered water (Unfiltered$_1$ in Fig. 6), flowing approximately at a rate of 5 L per minute. Two minutes after start, the electrovalve was activated, forcing the water through the 0.2 μm filter (T_0 in Fig. 6). The electrovalve activation also translates into a flow reduction to 1 L per minute (Fig. 6a). Since b4bbo volume is approximately 8 L (Table 3), the process of changing the water lasted for 8 min in which the unfiltered water was pumped in, diluting the particle concentration. Then the electrovalve was activated again to force the seawater through the normal path, without filter (T_1 in Fig. 6). The acquisition continued for four more minutes with the water flowing again at the unfiltered rate of 5 L per minute (Unfiltered$_2$ in Fig. 6). Measurements acquired during Unfiltered$_2$ (minute 10–14) is compared with the initial
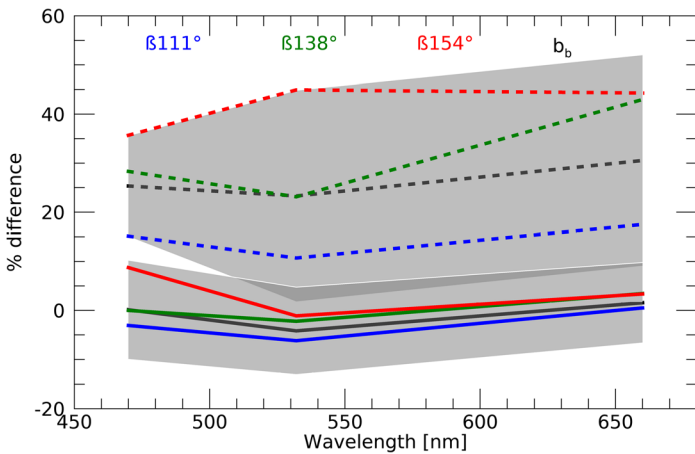
Fig 9. Median percent difference between continuous and cast mode acquisitions of VSF and b_b (black). Dashed lines indicate the measurements in continuous mode were performed without placing the cone in the b4bbo center, while continuous lines indicate the measurements with the cone in the b4bbo center. Shaded areas represent the ± 1 standard deviation for the two b_b measurements. Data used in this figure can be accessed at 10.5281/zenodo.4564781

Unfiltered$_1$ from which, in theory, the optical properties should not have changed significantly. Each acquisition sequence lasted 14 min.

Figure 6 provides an example of the acquisition started at 18:30 UTC of 1st June 2019. Obviously, the rate of water exchange into b4bbo is a function of the flowrate (Fig. 6a) and this is clearly visible from the steeper b_b slope after T_1 than after T_0 (Fig. 6b). Given the much smaller volume of

both c- and a-tubes (Table 3), the residence time of the water into the ACs is much shorter than into b4bbo as shown in (Fig. 6c), with the attenuation coefficient exhibiting a much faster response to the electrovalve switch. It is worth noting that, at T_1, b4bbo is not entirely replete of particles, as b_b values are still ~ 0.008 m^{-1} and ~ 0.005 m^{-1} in the blue and red bands, respectively, hence higher than the b_{bw} values of Fig. 5a (~ 0.004 m^{-1} and ~ 0.0016 m^{-1}). This experiment thus allows to mimic a sharp transition between waters characterized by different attenuation coefficients such as oceanic fronts. In Fig. 6b, the horizontal colored dashed lines indicate the median value of the b_b before switching to filtered water (Unfiltered$_1$) and serves as a reference to determine to which extent the water into b4bbo has renewed after switching to unfiltered water (Unfiltered$_2$).

Seawater residence time in b4bbo was estimated as the time, starting from T_1 in Fig. 6b, needed for the difference between each acquisition of b_b (Unfiltered$_2$) and the average b_b (Unfiltered$_1$) to fall within the standard deviation of b_b (Unfiltered$_1$). In the experiment shown in Fig. 6, it took roughly 4 min and 20 L of new water for bb (Unfiltered$_2$) to be comparable with bb (Unfiltered$_1$). A more robust estimate of the seawater residence time is provided in Fig. 7, which summarizes the outcome of the entire set of 16 experiments. On average, the residence time ranges between 100 and 160 s or alternatively an amount of 8–13 L are needed to significantly replace the water into b4bbo (Fig. 7). Other than b4bbo shape and tangential water inlet, this efficiency is also linked to the distance (maximized as much as possible) between the water in- and outlet.

Table 4. Statistics of the comparison between continuous and cast modes for both VSF and bb, without the cone in the center of b4bbo ($N = 23$). Details can be found in Section 1.3.

Variable	λ	θ	MedCo	MedCa	Intercept	Slope	r^2	RMSD	Bias	RPD	APD
Units	nm	Degrees	m^{-1} sr^{-1} $\times 10^{-3}$	m^{-1} sr^{-1} $\times 10^{-3}$	m^{-1} sr^{-1} $\times 10^{-3}$			m^{-1} sr^{-1} $\times 10^{-3}$	m^{-1} sr^{-1} $\times 10^{-3}$	%	%
β	470	111	4.61	4.07	0.3	1.03	0.95	0.53	0.45	14	14
		138	4.01	3.35	0.6	1.07	0.88	0.90	0.81	33	33
		154	4.96	3.88	0.9	1.11	0.89	1.30	1.23	43	43
	532	111	3.78	3.55	0.3	1.08	0.98	0.34	0.29	10	10
		138	2.74	2.46	0.4	1.25	0.96	0.50	0.47	25	25
		154	3.92	3.19	0.3	1.04	0.89	1.19	1.11	45	45
	660	111	3.13	2.82	0.4	1.22	0.93	0.45	0.38	17	17
		138	2.50	1.75	3.9	1.06	0.85	0.76	0.72	50	50
		154	2.55	1.82	2.2	1.09	0.89	0.78	0.74	47	47
Units	Nm	Degrees	m^{-1} x10^{-3}	m^{-1} x10^{-3}	m^{-1} x10^{-3}			m^{-1} x10^{-3}	m^{-1} x10^{-3}	%	%
b_b	470		0.03	0.02	0.3	1.00	0.93	5.44	5.02	28	28
	532		0.02	0.02	0.5	1.15	0.95	4.10	3.80	24	24
	660		0.02	0.01	2.5	1.09	0.92	3.89	3.65	32	32

Table 5. Statistics of the comparison between continuous and cast modes for both VSF and bb, with the cone in the center of b4bbo ($N = 32$). Details can be found in Section 1.3.

Variable	λ	θ	MedCo	MedCa	Intercept	Slope	r^2	RMSD	Bias	RPD	APD
Units	nm	Degrees	$m^{-1} sr^{-1}$ $\times 10^{-3}$	$m^{-1} sr^{-1}$ $\times 10^{-3}$	$m^{-1} sr^{-1}$ $\times 10^{-3}$			$m^{-1} sr^{-1}$ $\times 10^{-3}$	$m^{-1} sr^{-1}$ $\times 10^{-3}$	%	%
β	470	111	3.20	3.33	0.0	0.99	0.90	0.46	−0.10	−1	7
		138	2.38	2.32	0.0	0.99	0.93	0.28	−0.02	0	6
		154	3.05	2.78	0.2	1.01	0.94	0.38	0.25	8	9
	532	111	2.72	2.97	−0.2	1.08	0.91	0.45	−0.18	−5	9
		138	1.70	1.71	−0.2	1.09	0.93	0.26	0.01	0	6
		154	2.14	2.14	0.0	1.02	0.95	0.29	0.03	0	5
	660	111	2.21	2.21	−0.1	1.11	0.96	0.22	0.07	3	6
		138	1.52	1.46	0.2	1.00	0.95	0.18	0.09	5	6
		154	1.64	1.54	−1.4	1.05	0.92	0.27	0.12	6	7
Units	nm	Degrees	$m^{-1} \times 10^{-3}$	$m^{-1} \times 10^{-3}$	$m^{-1} \times 10^{-3}$			$m^{-1} \times 10^{-3}$	$m^{-1} \times 10^{-3}$	%	%
b_b	470		0.02	0.02	−0.3	1.03	0.92	2.15	0.25	1	6
	532		0.01	0.01	0.0	1.04	0.93	2.07	−0.40	−2	7
	660		0.01	0.01	−0.1	1.05	0.95	1.34	0.55	4	6

We conclude that the obtained estimation of the rate of water exchange into b4bbo associated with a vessel speed of 10 knots (roughly 300 m/min) make this system suitable for an efficient and robust pixel scale Cal/Val activity of OC data. Obviously, if the satellite pixel resolution that these data are targeted to is higher, vessel speed must be reduced or the water flow into the system increased.

Continuous vs. cast mode measurement: CoCa comparison

One way to ensure the continuous data are acquired correctly without any unknown bias is to periodically compare them with data acquired in cast mode. The cast mode is the way the IOP package used here was designed to be operated and here it is used as reference. To this aim, the comparison is performed on couples of cast and continuous measurements acquired consecutively.

During the first part of the cruise (7th through 23rd May 2019), b4bbo was used without the deflecting cone at the bottom, as shown in Fig. 3. The analysis made onboard during data acquisitions identified a significant bias between continuous and cast measurements. This analysis highlighted that the discrepancy was consistently distributed across all wavelengths and slightly increasing toward higher angles (Fig. 8a,c). Adding the cone to b4bbo significantly reduced this bias (Fig. 8b,d). Using the same set of observations as Fig. 8, Fig. 9 shows bias reduction to be evident and significant, with the uncertainty in b_b estimates reduced from 23%–30% to −4%–1% RPD. Tables 4 and 5 provide the statistics associated with the plots of Figs. 8 and 9. It is further clear that the addition of the cone to

system design did improve the quality of the continuous measurements by significantly reducing both the bias and the root mean square difference between cast and continuous measurements.

Summary and recommendations

In this work, we have documented the system characterization of the continuous and cast mode approaches for particle backscattering measurements in surface ocean. The system described here differs from those already documented in the literature (Boss et al. 2019) in two main aspects:

- The instrumentation generally used in underway systems measures VSF or b_b with simpler geometry, i.e., three bands and one angle (Dall'Olmo et al. 2009). Given their shape and consequently their sampling mode, these commercial instrumentations are much easier to implement into an underway flow-through system. However, more complex sensing geometry (WetLabs ECO-VSF3) allows for a more accurate estimation of the volume scattering function.
- The system presented here is designed to measure b_b in continuous and cast modes with the same instrumentation. This has several benefits, the two measurement types do not require a second set of instruments, which can obviously be used for cross-calibration and validation, if available. With a little effort of data processing, the CoCa system allows an early issue identification as we have shown here in this work when the placement of a reflecting cone at the bottom of the bucket resulted in a clear improvement in data quality.

The only drawback of this approach is given by the fact that the system, anytime is used in cast mode, has somehow to be emptied and filled again soon after the cast or at least be reset, as the presence of bubbles after maintenance is almost unavoidable. To reduce useless efforts, one can plan the cast measurements in correspondence of the daily system cleaning (Boss et al. 2019) as it was performed during the BioOpt 2019 cruise. Finally, in analogy to almost all automatic data systems, a full and detailed logging method is strongly recommended, allowing a better description of variables of interest for multidisciplinary applications.

This is, to the best of our knowledge, the first time an ECO-VSF3 is used into an underway system. Moreover, given the benefits of our approach, we recommend analog system designs for other b_b sensors.

The outcome of this exercise is that the contribution of b4bbo to the b_b measurements is negligible for the types of waters encountered during the BioOpt 2019 cruise. The laboratory experiment carried out during this work suggests that in optically thinner waters b4bbo could contribute more to the measured signal: this will constitute the matter of future research and development on this topic.

Furthermore, to avoid the current drop in flowrate under filtering conditions and to ensure flow stability, we plan to include two filter cartridges of 0.2 μm and 5 μm, set in series, with associated housing: Flotrex AP (absolute filter made of pure polypropylene microfibers) from SUEZ water technology (https://www.suezwatertechnologies.com/products/flotrex-pleated-cartridge-filters). The 5 μm pre-filter finds its best applicability in turbid waters to prevent the 0.2 μm filter from clogging. The flow stability is ensured by the roughly five times larger filtration area of the new filters (6400 cm^2 for the 0.2 μm and 6000 for the 5 μm against those used in this work 1350 cm^2). A further improvement could be setting more filters in parallel, rather than in series. This will in turn reduce the time required to deplete b4bbo with filtered water, thus allowing the subtraction of water and CDOM components from the total IOPs (Dall'Olmo et al. 2009; Slade et al. 2010). This technique will thus be used to correct for background effects in b4bbo, instrumental drifts in ECO-VSF3 and ACs, or ACs sensitivity to external parameters such as temperature or pressure.

References

Antoine, D., F. d'Ortenzio, S. B. Hooker, G. Bécu, B. Gentili, D. Tailliez, and A. J. Scott. 2008. Assessment of uncertainty in the ocean reflectance determined by three satellite ocean color sensors (MERIS, SeaWiFS and MODIS-A) at an off-shore site in the Mediterranean Sea (BOUSSOLE project). J. Geophys. Res. Ocean. **113**. doi:10.1029/2007JC004472

Banks, A. C., Vendt, R., Alikas, K., Bialek, A., Kuusk, J., Lerebourg, C., Ruddick, K., Tilstone, G., Vabson, V., Donlon, C., Casal, T. 2020. Fiducial reference measurements for satellite Ocean Colour (FRM4SOC). Remote Sens. **12**: 1322. doi:10.3390/RS12081322

Behrenfeld, M. J., and E. Boss. 2003. The beam attenuation to chlorophyll ratio: An optical index of phytoplankton physiology in the surface ocean? Deep Res. Part I Oceanogr. Res. Pap. **50**: 1537–1549. doi:10.1016/j.dsr.2003.09.002

Behrenfeld, M., E. Boss, D. Siegel, and M. D. Shea. 2005. Carbon-based ocean productivity and phytoplankton physiology from space. Global Biogeochem. Cycles **19**: GB1006. doi:10.1029/2004GB002299

Bellacicco, M., and others. 2019. Global variability of optical backscattering by non-algal particles from a biogeochemical-Argo data set. Geophys. Res. Lett. **46**: 9767–9776. doi:10.1029/2019GL084078

Bellacicco, M., G. Volpe, S. Colella, J. Pitarch, and R. Santoleri. 2016. Remote sensing of environment influence of photoacclimation on the phytoplankton seasonal cycle in the Mediterranean Sea as seen by satellite. Remote Sens. Environ. **184**: 595–604. doi:10.1016/j.rse.2016.08.004

Boss, E., and others. 2019. *In* A. R. Neeley and A. Mannino [eds.], IOCCG ocean optics and biogeochemistry protocols for satellite ocean colour sensor validation, v. **4.0**. Dartmouth, NS: IOCCG.

Clark, D. K., and others. 2003. MOBY, a radiometric buoy for performance monitoring and vicarious calibration of satellite ocean color sensors: Measurement and data analysis protocols, p. 139. *In* J. L. Mueller, G. S. Fargion, and C. R. McClain [eds.], Ocean optics protocols for satellite ocean color sensor validation, NASA Tech. Memo. 2003–211621/Rev4, v. **VI**. Greenbelt, MD: NASA GSFC.

Dall'Olmo, G., T. K. Westberry, M. J. Behrenfeld, E. Boss, and W. H. Slade. 2009. Significant contribution of large particles to optical backscattering in the open ocean. Biogeosciences **6**: 947–967. doi:10.5194/bg-6-947-2009

Hénin, C., and J. Grelet. 1996. A merchant ship thermo-salinograph network in the Pacific Ocean. Deep Sea Res. Part I Oceanogr. Res. Pap. **43**: 1833–1855. doi:10.1016/S0967-0637(96)00084-2

Kostadinov, T. S., D. A. Siegel, and S. Maritorena. 2009. Retrieval of the particle size distribution from satellite ocean color observations. J. Geophys. Res. Oceans **114**. doi:10.1029/2009JC005303

Liberti, G. L., and others. 2020. European radiometry buoy and infrastructure (EURYBIA): A contribution to the design of the European copernicus infrastructure for ocean colour system vicarious calibration. Remote Sens. (Basel) **12**: 1178. doi:10.3390/rs12071178

Loisel, H., J.-M. Nicolas, A. Sciandra, D. Stramski, and A. Poteau. 2006. Spectral dependency of optical backscattering by marine particles from satellite remote sensing of the global ocean. J. Geophys. Res. **111**: C09024. doi:10.1029/2005JC003367

Lorenzen, C. J. 1966. A method for the continuous measurement of in vivo chlorophyll concentration. Deep Sea Res. **13**: 223–227. doi:10.1016/0011-7471(66)91102-8

Martinez-Vicente, M., G. Dall'Olmo, G. Tarran, E. Boss, and S. Sathyendranath. 2013. Optical backscattering is correlated with phytoplankton carbon across the Atlantic Ocean. Geophys. Res. Lett. **40**: 1154–1158. doi:10.1002/grl.50252

Slade, W. H., E. Boss, G. Dall'Olmo, M. R. Langner, J. Loftin, M. J. Behrenfeld, C. Roesler, and T. K. Westberry. 2010. Underway and moored methods for improving accuracy in measurement of spectral particulate absorption and attenuation. J. Atmos. Oceanic Tech. **27**: 1733–1746. doi:10.1175/2010JTECHO755.1

Sullivan, J. M., M. S. Twardowski, J. Ronald, V. Zaneveld, and C. C. Moore. 2012. Measuring optical backscattering in water, p. 189–224. *In* A. A. Kokhanovsky [ed.], Light scattering reviews, Springer. doi:10.1007/978-3-642-15531-4

Valente, A., and others. 2016. A compilation of global bio-optical in situ data for ocean-colour satellite applications. Earth Syst. Sci. Data **8**: 235–252. doi:10.5194/essd-11-1037-2019

Volpe G., and others (2018). *IOPs continuous measurements for ocean monitoring and calibration and validation of satellite data*. Poster presented at the Ocean Science Meeting 2018, 11–16 February 2018, Portland, OR, USA.

Westberry, T., M. Behrenfeld, D. Siegel, and E. Boss. 2008. Carbon-based primary productivity modeling with vertically resolved photoacclimation. Global Biogeochem. Cycles **22**: GB2024. doi:10.1029/2007GB003078

Zhang, X., L. Hu, and M.-X. He. 2009. Scattering by pure seawater: Effect of salinity. Opt. Express **17**: 5698–5710. doi:10.1364/OE.17.005698

Zibordi, G., and others. 2015. System vicarious calibration for ocean color climate change applications: Requirements for in-situ data. Remote Sens. Environ. **159**: 361–369. doi:10.1016/j.rse.2014.12.015

Conflict of interest

None declared.